Article:
Alghamdi, N., Alqahtani, Z., Zhou, C. et al. (2020) Sensing aromatic pollutants in water with catalyst-sensitized water-gated transistor. Chemical Papers, 74 (12). pp. 4169-4180. ISSN: 0366-6352

https://doi.org/10.1007/s11696-020-01212-3

Sensing aromatic pollutants in water with catalyst-sensitized water-gated transistor

Nawal Alghamdi*[1,2] Zahrah Alqahtani[1,3], Changyan Zhou[4], Naoko Sano[5], Marco Conte[4], and Martin Grell[1,6]

[1]Physics and Astronomy, University of Sheffield, Hicks Building, Hounsfield Rd, Sheffield S3 7RH, UK
[2]Department of Physics, University of Tabuk, King Fahad Road, Tabuk 47731, Saudi Arabia
[3]Department of Physics, University of Taif, Taif-Al-Haweiah 21974, Saudi Arabia
[4]Department of Chemistry, Dainton Building, University of Sheffield, Sheffield, S3 7HF, UK
[5]Nara Women's University, Nisi-machi, Kita Uoya, Nara, 630-8506, Japan
[6]Llyfrgell Bangor, Ffordd Gwynedd, Bangor, LL57 1DT, UK

*Corresponding author, nhalghamdi1@sheffield.ac.uk

Abstract

Some materials that are active heterogeneous catalysts for the breakdown of non- ionic aromatic solutes in water are found to act as potentiometric sensitizers for same solutes. As an example, here the aromatic water pollutant, benzyl alcohol, was sensed with a limit-of- detection (LoD) below its potability limit of 19 μM. Our findings are rationalized on the grounds that both catalysis and sensing rely on adhesion of analyte/substrate on the sensitizer / catalyst. Specifically, a set of powdered transition metal doped zeolites and related frameworks that catalyze the oxidation of waterborne aromatic pollutants were dispersed in phase transfer matrices. Matrices were introduced into water-gated thin film transistors (WGTFTs) that act as potentiometric transducers. Potentiometric sensing of non-ionic waterborne pollutants is limited to molecules with a 'free' molecular dipole, *i.e.* a dipole that is not locked in the molecular plane. The present work establishes an application for catalysts beyond catalysis itself. The use of catalysts as sensitizers is recommended for wider uptake and in reverse, to screen candidate catalysts.

Keywords: WGTFT, zeolite, benzyl alcohol, sensor, catalyst

Introduction

The first step in heterogeneous catalysis is the adsorption of a 'substrate', *i.e.* a molecule that is meant to be catalyzed, from solution onto the surface of a solid catalyst. Adsorption often is highly selective (Friend et al. 2017; Medford et al. 2015). If the initial adsorption of substrate onto a catalyst surface can be transduced into a physical (*e.g.* electrical) signal, then a material known to be a catalyst for a particular substrate would also act as a selective receptor or 'sensitizer' in a sensor for this substrate, which then would be called the sensor's 'analyte'. Such a sensor will be effective even below the temperature required for a catalyst to be active, as adsorption already occurs at lower temperatures. The present work demonstrates this concept on the example of an aromatic alcohol, benzyl alcohol, as substrate/analyte in aqueous solution. Transition metal doped zeolites and similar frameworks acted as sensitizer. As the transducer for adsorption, a water-gated thin film transistor (WGTFT) was employed.

Transition metal doped zeolites are commonly applied in heterogeneous catalysis (Friend et al. 2017 ; Medford et al. 2015; Čejka et al. 2016) and are used in the finely powdered form *e.g*. for the treatment of water polluted with aromatic contaminants (Inchaurrondo et al. 2012 ; Rahman et al. 2018; Valkaj et al. 2011). In addition, such catalysts have been used as sensitizers in amperometric and voltammetric sensors for waterborne analytes (Rahman et al. 2018 ; Rahman et al. 2016; Rostami et al. 2017) and also in potentiometric gas sensors (Sahner et al. 2008). However, they have not previously been reported in potentiometric sensors for waterborne analytes.

Here, first the catalytic activity of a number of transition-metal doped zeolite 'candidate' sensitizers was confirmed by selecting appropriate non-ionic aromatic water pollutants, namely: phenol, benzyl alcohol, and toluene. It should be noted that in our case we don't aim to trap or exchange any of these pollutants within the zeolite framework, but rather to catalytically degrade them by oxidizing them to CO_2, water or ketones, by using H_2O_2 or O_2 as oxidizing agents. For our sensing tests instead, phase transfer membranes were filled with such powder zeolite catalysts, and introduced into a novel potentiometric sensor concept for waterborne analytes, the water-gated thin film transistor (WGTFT). In this

context, our membranes act as a medium to allow the measurement of electrical properties of our materials, but again with no ion exchange process involved in our experiments. Since its introduction in 2010 (Kergoat et al. 2010), the WGTFT has emerged as a useful potentiometric transducer of membrane potentials, e.g. for ion-selective membranes (Al Baroot and Grell 2019; Melzer et al. 2014; Schmoltner et al. 2013). In the WGTFT, a gate voltage is communicated to the TFT channel across the aqueous medium via pairs of electric double layers (EDLs) forming at the gate electrode / water, and water / channel, interfaces. This communication can easily bridge macroscopic (millimeter or more) distances while still maintaining high specific capacitance (>1 μF/cm^2). When a membrane is inserted in the aqueous medium between the gate electrode and the channel, any membrane potential $V_M(c)$ that may develop under analyte concentration c is added to the applied gate voltage. Membrane potentials are therefore transduced into a corresponding shift of WGTFT threshold voltage, $\Delta V_{th}(c)$. Phase transfer membranes typically were sensitized with organic macrocycles as ionophores. Macrocycles selectively capture a specific ion in their central cavity, thus in the presence of 'target' (analyte) ion, charge accumulates in the membrane. In that case, membrane potential, $V_M(c)$, follows a Nikolsky-Eisenman (modified Nernstian) characteristic (Al Baroot and Grell 2019; Melzer et al. 2014 ; Schmoltner et al. 2013). Recently, some of the present authors have instead introduced ion exchanging (rather than ion capturing) inorganic ionophores into WGTFT membranes (Alghamdi et al. 2019; Alqahtani et al. 2020). Selective response with low limit- of- detection (LoD) was demonstrated for Cs^+, Pb^{2+}, and Cu^{2+} (Alghamdi et al. 2019 ; Alqahtani et al. 2020), but membrane potential $V_M(c)$ followed a different characteristic, namely a Langmuir-Freundlich (LF) adsorption isotherm, eq. 1:

(eq. 1) $$V_M(c) = \Delta V_{th}(c) = \Delta V_{th}(\text{sat})\ (Kc)^{\beta} / [(Kc)^{\beta} + 1]$$

K quantifies the strength of the interaction between a sorption site and the sorbate, $\beta \leq 1$ quantifies inhomogeneity between sorption sites ($\beta = 1$, K for all sorption sites is equal,

giving the classic Langmuir isotherm as a special case). $\Delta V_{th}(sat)$ is a saturation value for membrane potential / threshold shift under large c. A characteristic concentration $c_{1/2}$ is given by $\Delta V_{th}(c_{1/2}) = ½\ \Delta V_{th}(sat)$; $c_{1/2} = 1/K$ independent of β. The different characteristics are assigned to the different origin of membrane potential: while macrocycles accumulate charge in the membrane, ion exchange changes the dipole moment, leading to a polarization (Alghamdi et al. 2019; Alqahtani et al. 2020).

The present work is inspired by the observation that changes in dipole moment under ion exchange can generate large membrane potentials without the net charging of the membrane. While phase transfer membrane sensitized WGTFTs have so far only been used as ion sensors, polarization should enable the WGTFT-transduced detection of non-ionic solutes, as well: When a non-ionic, organic substrate / water pollutant that carries a molecular dipole adsorbs from the aqueous phase onto the surface of a catalyst, this should also lead to a change in the catalyst's surface polarization. Consequently, phase transfer membranes sensitized with powdered catalyst grains should develop a membrane potential under exposure to a substrate. The WGTFT should then transduce membrane potential into a threshold shift. The present report shows that some zeolite-catalyst loaded membranes indeed shift WGTFT threshold under water polluted with benzyl alcohol, but not under toluene or phenol pollution. This report therefore establishes a new application for catalysts beyond catalysis itself, namely as sensitizers in sensors for water pollution, which is recommended for wider uptake. The potentiometric sensing mechanism is discussed to establish criteria which type of non-ionic aromatic pollutants can be sensed in this way at all. Further, the relationship between catalytic activity, and sensing performance is discussed.

2. Experimental

a.) Selection and modification of Zeolites and related materials:

Within this study, we investigated 10 candidate catalysts/sensitizers which either were derived from common 'parent' zeolites (aluminosilicates) namely ZSM-5 (belonging to the MFI framework, a structure consisting of two parallel channels), and Zeolite type 13X and zeolite Y (belonging to the FAU framework, consisting of a cage structure), or were derived from mesoporous silicate 'parents' lacking aluminum centers that are frequently used as support materials for catalysts, namely MCM-41 and SBA-15. Note, MCM-41 and SBA-15 are not strictly zeolites but similar mesoporous silicate frameworks that lack the aluminum centers of zeolites with their associated Brønsted acid properties. However, due to their otherwise similar structure, we here will summarily refer to all frameworks as 'zeolites' rather than 'zeolite- and related frameworks'. Parent materials were sourced commercially as fine powders (ThermoFisher Scientific, 45879 zeolite ZSM-5 ammonium; A10378 Molecular sieves, 13X, powder; 45866 Zeolite Y, hydrogen; Sigma-Aldrich, Silica, mesostructured MCM-41 type (hexagonal) ; mesostructured SBA-15, 99% trace metals basis) to represent a range of different pore sizes, aluminium contents (including zero for MCM-41, SBA-15) and surface areas. These parameters affect the growth of metal nanoparticles (Zhao et al. 2011) under the subsequent doping protocols described below. Usually, the larger the surface area, the smaller and more isolated are the resultant dopant metal nanoparticles (Wilde et al. 2019). Surface area and pore size may also introduce diffusion effects which can influence catalytic activity. The framework's molar Al : Si ratio affects the stability of the framework and its acidity (the higher the Al : Si ratio, the more acidic a zeolite is), which is a key characteristic for catalytic activity (Xu et al. 2007). Zeolite frameworks were then modified by doping with 1-1.5 wt% of transition metals Cu, Fe, or Mn. These are capable to catalyze the decomposition of organic pollutants like phenol to CO_2 and water in the presence of molecular oxygen or peroxides (Maduna et al. 2007 ; Meng 2013), or to oxidize alcohols to ketones. Transition metal doping was by different protocols: wetness impregnation (WI); ion exchange (IE); and deposition precipitation (DP). WI (Conte et al. 2012) leads to relatively large clusters (> 20 nm) of CuO mostly outside the pores of the zeolite. IE instead leads to smaller (usually < 5 nm) CuO clusters or to the exchange of Al centers with Cu centers, or other metals

(Barrer et al. 1976). DP can lead to the formation of mixed metal oxide CuO/Cu_2O species in the range of 10 nm or lower (Gurbani et al. 2009). Details on the doping protocols employed here are in the supplementary information, part 1. A numbered list of the resulting materials used here is in table 1.

Table 1: The 10 materials studied here. Aluminosilicate zeolites: ZSM-5, X, Y, and highly silicate zeolites MCM, and SBA. The standard notation used denotes the respective zeolite framework: ZSM-5, Zeolite Socony Mobil 5 (ZSM-5) (ThermoFisher Scientific, zeolite ZSM-5 ammonium form), zeolite type Y (Y), zeolite type 13X (13X) (ThermoFisher Scientific, Molecular sieves, 13X, powder; ThermoFisher Scientific, 45866 Zeolite Y, hydrogen), highly silicate zeolites: Mobil Composition of Matter (MCM-41) (Sigma-Aldrich, Silica, mesostructured MCM-41 type (hexagonal), Santa Barbara Amorphous-15 (SBA-15)) (Sigma-Aldrich, Silica, mesostructured SBA-15, 99% trace metals basis). All the zeolites are used in acidic form, with the exception of No.4, where an ammonium zeolite precursor (NH_4-ZSM5) was used. WI = wetness impregnation, IE = ion exchange, DP = deposition precipitation.

Zeolite No.	Composition (wt%) / Preparation	Si : Al molar ratio
1	1% Cu/ZSM-5-WI	46 : 1
2	1.5% Cu/ZSM-5-IE	46 : 1
3	1% Cu/ZSM-5-DP	46 : 1
4	1% Cu/NH_4-ZSM-5-WI	46 : 1
5	1% Cu/13X-WI	1.2 : 1
6	1.5% Cu/Y-IE	11 : 1
7	1% Fe/ZSM-5-WI	46 : 1

8	1% Fe/MCM-41-WI	1 : 0
9	1% Fe/SBA-15-WI	1 : 0
10	1% Mn/ZSM-5-WI	46 : 1

Wetness impregnation (WI) and deposition precipitation (DP) protocols are expected to lead to the formation of small metal oxide clusters on the external surface of the zeolite crystals (Meng et al. 2013), known as ‘extra-framework’ species. Such procedure should not lead to any change in lattice parameters and unit cell volume of the zeolite. Ion exchange protocols instead can lead to intra-framework species (Lopez-Sanchez et al. 2012), that is the doping metal replaces some Al centers within the Si-O-Al framework. The latter effect can lead to changes of lattice parameters. All of the materials in table 1 as well as the ‘parent materials’ prior to modification were therefore characterized by powder X-ray diffraction (supplementary section S2.a, Figures S1 to S6), and where appropriate, also by X-ray photoelectron spectroscopy (XPS) (supplementary section S2.b, Fig.s S7 and S8). In summary, all materials present extra-framework species, although material No. 6, a Cu-doped Y zeolite obtained by ion exchange, shows the largest change in unit cell volume due to doping, albeit the change still is rather small (0.5%). This small contraction could suggest the incorporation of some Cu into the aluminum framework of the zeolite. Also, only material No. 6 showed some copper in oxidation state +I (namely, 23%) rather than +II.

b.) Selection of analytes and solution preparation

To allow systematic comparison, sensing was tested on dilute solutions of three example aromatic water pollutants: benzyl alcohol, phenol, and toluene, shown in Fig. 1a, as examples of water pollutants. All three candidate analytes consist of a rigid benzene ring with one substitution, hence adhesion should be similar for all with any difference to be ascribed to the only different functional group. On the other hand, due to the different substitutions, the three molecules show very different molecular dipoles. The magnitude

of dipole moments ranges from strong to weak: benzyl alcohol, 1.7 Debye (D), phenol 1.5 D, and toluene 0.2 D, respectively (Schaefer et al. 1989; Pople and Gordon 1967). Further, benzyl alcohol has a dipole at the pendant -OH group that can rotate out of the plane of the benzene ring around the dihedral angle of the saturated carbon-carbon bond that links it to the benzene ring. Phenol also shows an -OH dipole but this is fixed in the plane of the ring as it is attached without 'spacer'. Toluene shows (almost) no dipole from the pendant non-polar methyl group. Test solutions of benzyl alcohol and phenol were prepared by diluting 1 mM stock solutions. For toluene, a saturated stock solution was prepared by mixing an excess of toluene with water, stirring for 24 hours then leaving for 2 days in a separating funnel to ensure separation, and drawing saturated solution of toluene in water from the funnel. According to (Polak and Lu 1973), at ambient temperature that corresponds to 30 mM. A saturated toluene solution was then diluted to make test solutions.

c.) Catalytic activity measurements

Before testing zeolites 1 to 10 as potential sensitizers in WGTFT sensors for the above three candidate analytes, catalytic activity of zeolites for the oxidation of these same molecules was established when they are considered as substrates.

Catalytic tests for phenol oxidation were carried out by dispersing the solid catalyst in an aqueous solution containing 10.6 mM of phenol and by adjusting catalyst amount or reactant in order to maintain a constant molar metal to substrate ratio (M : S) of 1:100. In a typical experiment, approximately 30 mg of catalyst and 50 mL of aqueous phenol solution were used. All catalytic tests were carried out in custom made glass 100 mL flasks equipped with a Young's valve - to be used as a batch reactor - at a constant reaction temperature of 80 ^{o}C. 0.76 mL of H_2O_2 (30%, VWR International) was added to the phenol solution as an oxidant when the temperature reached 80 ^{o}C to start the reaction. The flask containing the reaction mixture was inserted into a pre- heated temperature calibrated aluminum block for the desired reaction time, and equipped with a magnetic stirrer operating at 500 rpm. The reaction was quenched into an ice-water bath after 4 h. Analysis of the reaction mixture was carried out via HPLC using the

following analysis condition: XBridge C18 column, acetonitrile / 0.1% orthophosphoric acid solution with a ratio of 30%/70% (V/V) as mobile phase with a flow rate of 1 $mL \cdot min^{-1}$. Qualitative and quantitative characterization of the reaction mixture was carried out by comparison to standard solutions in the range 10 to 1000 mg L^{-1} of: phenol, hydroquinone, *p*-benzoquinone, catechol, maleic acid, malonic acid, acetic acid, and formic acid. CO_2 amount was calculated from the carbon mass balance for these products, and validated via total organic carbon determinations.

For catalytic activity tests on benzyl alcohol as substrate, the catalyst was dispersed in 5 mL of 277 mM of benzyl alcohol (Acros, 99%) solution adjusting the amount of substrate to a molar metal to substrate ratio of 1 : 100 for each catalyst with respect to the total amount of active metal. The reaction mixture was heated using a reflux condenser at 80 ^oC for 24 hours with a magnetic stirrer operating at 300 rpm at atmospheric pressure. Analysis of the reaction mixture to determine product selectivity and conversion was obtained via ^1H-NMR using a Bruker Avance IIIHD 400 spectrometer operating at 400 MHz. NMR spectra were collected using $CDCl_3$ as the solvent. Before NMR analysis, the reaction mixture was extracted with $CDCl_3$ for 1 h under stirring. After that, the subnatant solution was collected and analyzed. Chemical shifts were reported in parts per million (ppm) from tetramethylsilane (Gottlieb 1997). Partial NMR used for our quantification and identification of our compounds were: benzyl alcohol, δ (ppm): 7.83-7.28 (C_6H_5, m, 5H), 4.68 (CH_2, d, 2H, J = 5.3 Hz), 2.06 (OH, s broad, 1H); benzaldehyde, δ (ppm): 10.02 (CHO, s, 1H), 7.89-7.51 (C_6H_5, m, 5H), with: 7.89-7.87 (CH(*ortho*), m, 2H), 7.62-7.61 (CH(*para*), m, 1H), 7.54-7.51 (CH(*meta*), m, 2H).

d.) Phase transfer membrane preparation

To prepare PVC membranes 30 mg of PVC and 65 mg of plasticizer 2NPOE were dissolved in 3 mL of THF, which is a good solvent for all ingredients. All chemicals were purchased from Sigma Aldrich. Then, 7 mg of powdered zeolite as listed in table 1 were dispersed in 500 µL of such solution in a small vial and left overnight at room temperature to allow evaporation of THF. The resulting membranes were ~ 0.4 mm thick and were

then conditioned for one hour in DI water. Finally, the membrane was glued in between two plastic pools with epoxy, see Fig. 1b.

e.) Water- gated transistor preparation, setup, and measurement protocol

Transistor source/drain contact substrates were prepared by thermal evaporation of Au (100 nm) with Cr (10 nm) as adhesion layer onto clean quartz- coated glass substrates sourced from Ossila Ltd (order code S151) by a shadow mask. Each substrate contains 5 pairs of electrodes separated by channel with a length L = 30 µm and width W = 1 mm (W/L = 33.3). 4 sprays of 0.05 M $SnCl_4 \cdot 5H_2O$ dissolved in isopropanol were sprayed using an airbrush from 20 cm distance onto contact substrates preheated to 400 °C. Afterwards substrates were left on the hot plate for 30 min for full decomposition of tin chloride precursor into semiconducting SnO_2. Resulting film thickness was ~ 45 nm as determined with a Dektak surface profilometer, the bandgap of SnO_2 is 3.6 eV (Sankar et al. 2015). To test the response of membrane-sensitized WGTFTs to aromatic substrates, we used a 2- chamber design, similar to some previous workers (Arvand-Barmchi et al. 2003; Schmoltner et al. 2013), which is derived from the design of traditional potentiometric ion sensors, *e.g.* (Menon et al. 2011). The SnO_2 transistor substrate was in contact with DI water held in an 'inner' reference pool that is separated by the sensitized PVC membrane from a second, 'outer' sample pool. The outer pool is initially also filled with DI water, but this is then subsequently replaced with solutions of increasing analyte (substrate) concentrations, while the inner pool remains filled with DI water as analyte- free reference. The transistor is gated by a tungsten contact needle that is in contact with the sample solution in the outer pool. The setup is illustrated in Fig. 1b. As with all electrolyte- gated transistors, the potential applied to the gate contact is communicated to the semiconductor surface via interfacial electric double layers (EDLs). To record linear transfer characteristics, a small, constant positive voltage (+ 0.1 V) is applied to the drain contact while the source remains grounded. The drain current I_D then was recorded as a function of the voltage applied to the gate (gate Voltage, V_G). V_G is ramped from -0.6V → +0.8V. Drain current is low for negative or small positive gate voltage but rises linearly with gate voltage when the gate exceeds the threshold, V_{th}. However, the potential that applies at the semiconductor surface is different from the potential applied to the gate

needle by any membrane potential V_M in response to the substrate solution in the sample pool. Hence, the substrate-concentration dependent membrane potential $V_M(c)$ is transduced into a threshold shift $\Delta V_{th}(c)$, and the transfer characteristic shifts along the gate voltage axis (additional details concerning the threshold voltage analysis method in supplementary information section S3).

a.)

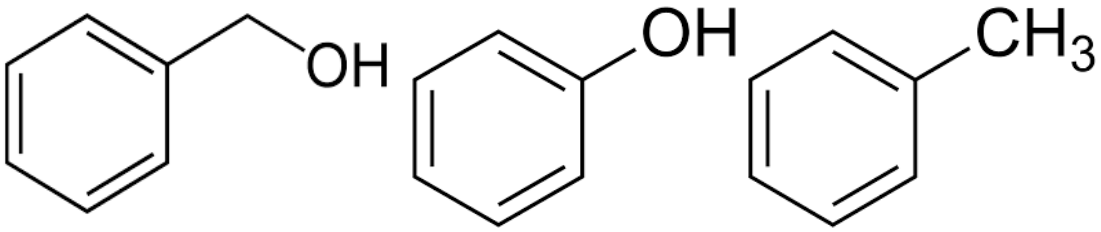

b.)

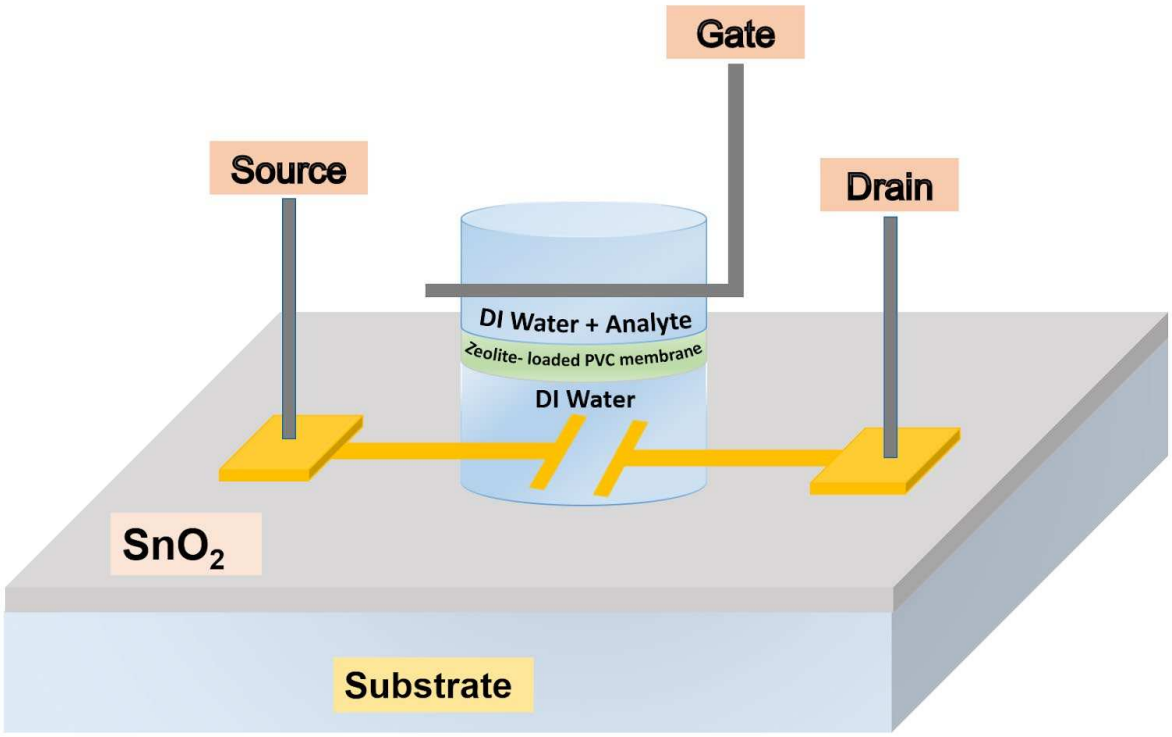

Fig. 1a: Chemical formulae of the three non- ionic aromatic analytes tested in this study, left to right: benzyl alcohol, phenol, and toluene. **b:** Schematic illustration of WGTFT

sensor setup. SnO_2 is spray pyrolyzed from tin chloride precursor over previously deposited Au / Cr adhesion layer source / drain contact pairs

f.) Data analysis

To determine threshold shift $\Delta V_{th}(c)$ quantitatively, recorded transfer characteristics at substrate concentration c > 0 were shifted along the V_G axis for best overlap with the c = 0 transfer characteristics (section S3 in supplementary information). The required shift for the best overlap was taken as $\Delta V_{th}(c)$. Resulting ΔV_{th} *vs* c response characteristics were fitted to the 'Langmuir Freundlich' (LF) isotherm, eq. 1, using the Origin 2018 non- linear fitting routine. Fitting returned β values not significantly different from 1 within the margin of error, therefore $\beta = 1$ was used for determination of limit- of- detection (LoD), *i.e.* the lowest concentration of an analyte (substrate) that can be detected with a particular zeolite in the WGTFT. Data were re- plotted in linearized form, $\Delta V_{th}(sat)\ (Kc + 1)$ *vs.* Kc. A straight line of the form $\Delta V_{th}(sat)\ (Kc + 1) = mKc + b$ was fitted, and linear fit parameters m and b +/- Δb evaluated by linear fitting routine in Origin software b overlapped with zero within +/- Δb, as expected. LoD was calculated from the common '3 errors' criterion,

(eq. 2) $Kc_{LoD} = 3\Delta b / m$

LoD is a key measure of sensor performance.

3. Results and discussion

a.) Catalytic activity

The catalytic activities of zeolites 1 to 10, as introduced in table 1, for the oxidation of aromatic water pollutants were determined following the protocol described in section 2c. Resulting activities are summarized in table 2, and they refer to the catalytic reactions reported eq.3 and eq.4, for phenol and benzyl alcohol oxidation respectively:

$C_6H_5\text{-}OH + 14\ H_2O_2 \rightarrow 6CO_2 + 17\ H_2O$ (eq. 3)

And

$C_6H_5\text{-}CH_2\text{-}OH + 1/2\ O_2 \rightarrow C_6H_5\text{-}CHO + H_2O$ (eq. 4)

Table 2: Summary of catalytic activity of zeolites 1 to 10 on substrates phenol (P) benzyl alcohol (BA). 'No.', zeolite number from table 1; (a) conversion rate calculated as initial rate over a reaction period of 20 min (as after 4 h all catalysts lead to completion), reaction conditions: 80 °C endogenous pressure (b) conversion rate after 24h, reaction conditions: 80 °C atmospheric pressure. For full experimental details see the supplementary information.

Zeolite No.	Composition / preparation	Benzyl alcohol conversion rate/ mM h^{-1} (b)	Phenol initial conversion rate/ mM h^{-1} (a)
1	1% Cu/ZSM-5-WI	0.09	0.65
2	1.5% Cu/ZSM-5-IE	0.12	1.43
3	1% Cu/ZSM-5-DP	0.16	0.43
4	1% Cu/NH4-ZSM-5-WI	0.01	0.38
5	1% Cu/13X-WI	0.20	1.59
6	1.5% Cu/Y-IE	0.17	1.59
7	1% Fe/ZSM-5-WI	0	0.34
8	1% Fe/MCM-41-WI	0	0.05
9	1% Fe/SBA-15-WI	0	1.54
10	1% Mn/ZSM-5-WI	0.24	< 0.01

Conversion rates for phenol are considerably higher than those of benzyl alcohol. The reason of this behavior is two-fold: (i) the oxidation of phenol is assisted by hydrogen peroxide, whereas the oxidation of benzyl alcohol is assisted by molecular oxygen, and (ii) the doping metals that have been selected for the zeolites are inherently more efficient

at hydrogen peroxide activation rather than molecular oxygen activation under our experimental conditions. Materials that are active for phenol oxidation may not be active for alcohol oxidation and vice-versa, because reaction mechanisms are different. An example of this are the Fe containing catalysts No.7 (1% Fe/ZSM), No.8 (1% Fe/MCM-41) , No.9 (1% Fe/SBA-15), which fail to catalyze benzyl alcohol oxidation. In fact, Fe-doped frameworks are known to be poor oxidizers for alcohols unless nitroxide species are added (Ma et al. 2011), and as such served as a control here. Fe-doped frameworks (No 7, and 8) also fail to catalyze phenol decomposition, but No. 9 is very active for phenol. Note though that sensing relies in the first step of catalysis only, namely adsorption to the catalyst surface, which nevertheless may be strong for benzyl alcohol despite of the lack of subsequent oxidation of the adsorbed substrate.

All candidates were also tested for catalytic activity on toluene (for the expected catalytic reaction reported in eq. 5) but there was no measurable catalysis of toluene at the conditions described in the supplementary information. It is known that the catalytic breakdown of toluene usually requires autoclave conditions (Brezinsky et al. 1984).

$C_6H_5\text{-}CH_3 + O_2 \rightarrow C_6H_5\text{-}CHO + H_2O$ (eq. 5)

b.) Sensing benzyl alcohol

First, all zeolites were tested for sensing of waterborne benzyl alcohol, an aromatic hydrocarbon with high solubility in water (> 277 mM). As a detailed example, we show results for WGTFTs sensitized with zeolite No. 3 (1% Cu/ZSM-5) membranes. Linear transfer characteristics under increasing benzyl alcohol concentration in the sample pool are shown in Fig. 2a.

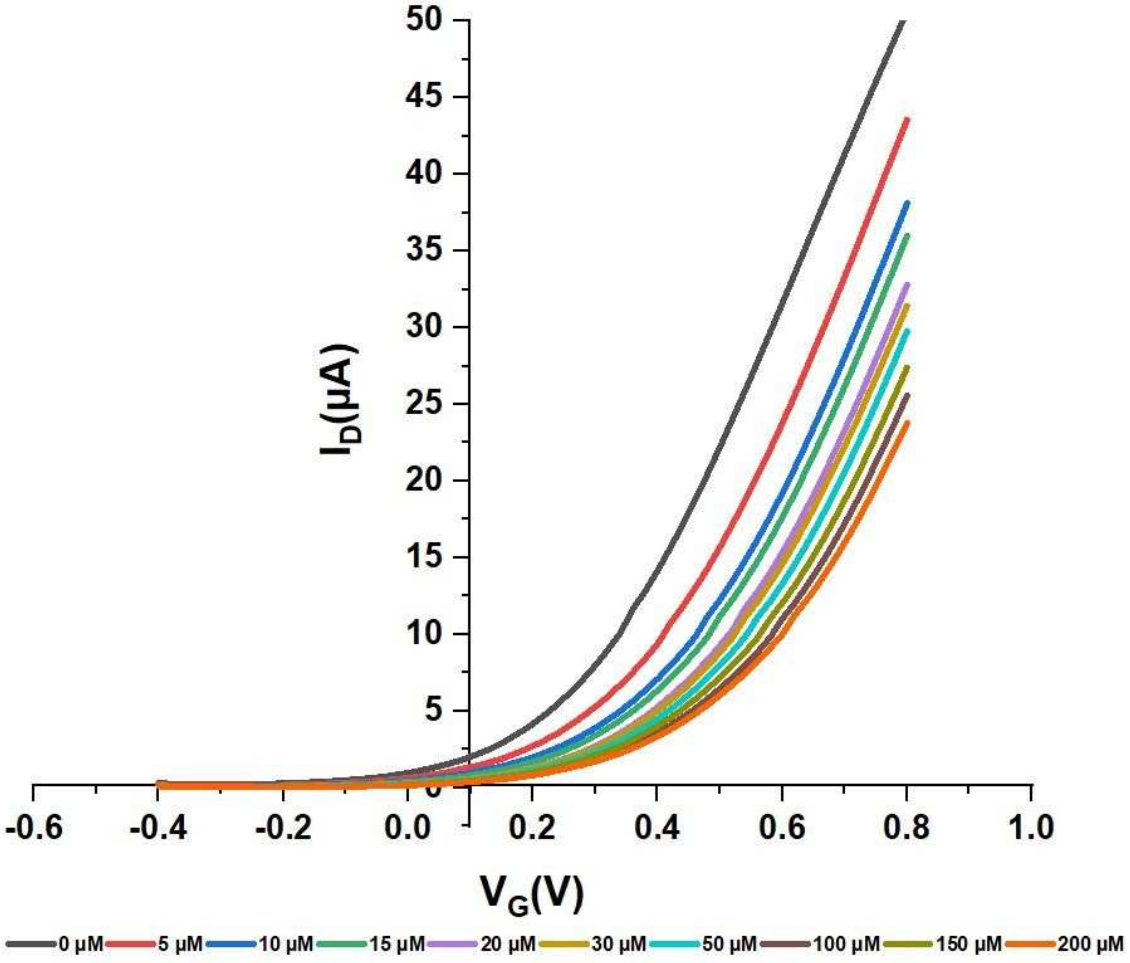
50
45
40
35
30
25
20
15
10
5
0
$I_D(\mu A)$
-0.6
-0.4
-0.2
0.0
0.2
0.4
0.6
0.8
1.0
$V_G(V)$
0 μM
5 μM
10 μM
15 μM
20 μM
30 μM
50 μM
100 μM
150 μM
200 μM

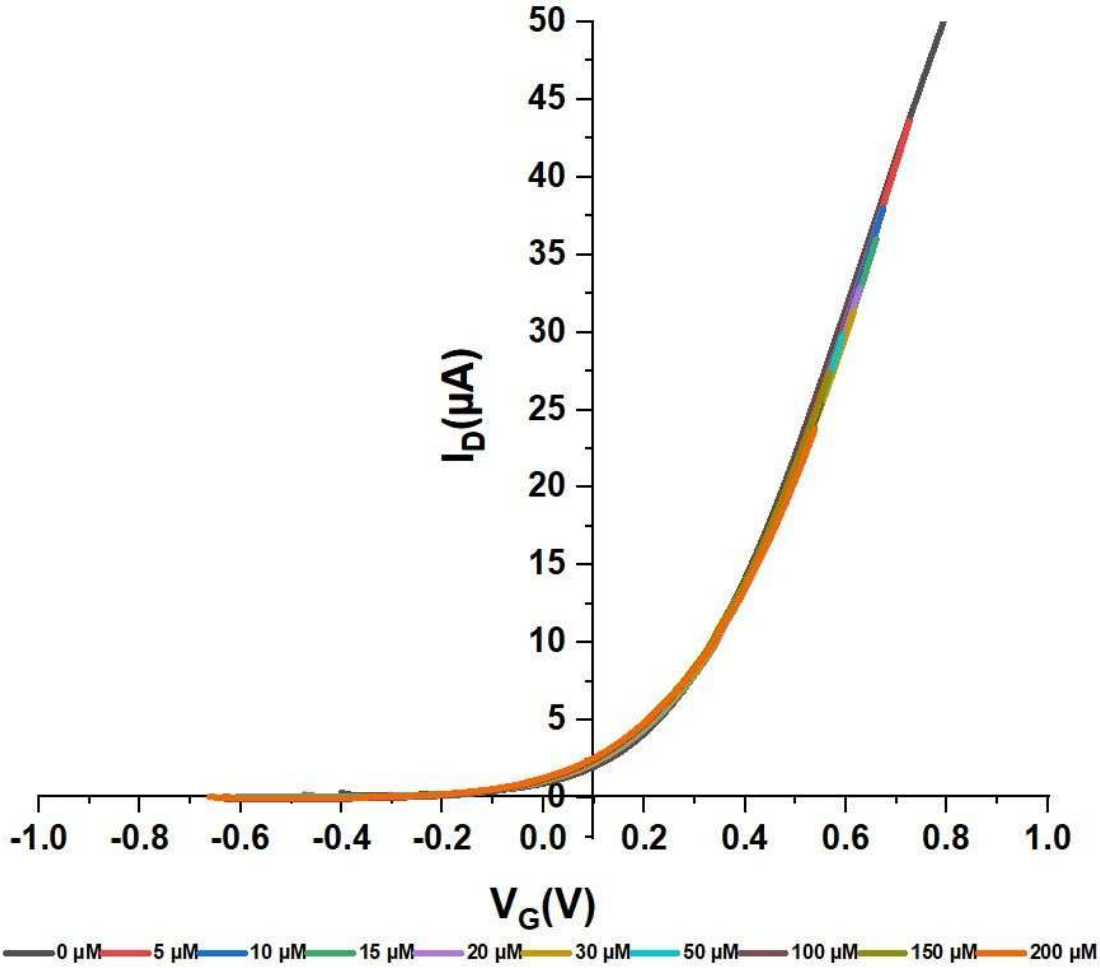

Fig 2a: Linear transfer characteristics for SnO_2 WGTFTs sensitized with zeolite No. 3 filled plasticized PVC membrane under water with increasing benzyl alcohol concentrations. **b:** Resulting 'master curve' after shifting all transfers along the V_G axis for best overlap with c = 0.

All transfer characteristics are similar but shift along the gate voltage axis towards larger voltages in response to a few micromolar or higher benzyl alcohol concentration in water. Threshold shift $\Delta V_{th}(c)$ is due to an increase of PVC membrane potential, $V_M(c)$, with increasing concentration c of the analyte, benzyl alcohol, in the sample pool. The membrane potential was assigned to the adsorption of dipolar benzyl alcohol molecules onto the surface of zeolite grains in the phase transfer membrane. A zeolite that was developed as a catalyst for aromatic pollutants in water also acts as a sensitizer for such a chemical at micromolar concentrations, even at ambient temperature where catalysis

will not yet be occurring. To quantify the threshold shift, all transfer characteristics are shifted along the gate voltage axis to match the c = 0 characteristics, as described in paragraph 2c. The resulting 'master curve' is shown in Fig. 2b. The good overlap into a single master curve confirms that the only impact of increasing analyte concentration in the sample pool is a membrane potential leading to a threshold shift, no other transistor parameter is affected.

Similar tests were carried out for all compounds listed in table 1 under benzyl alcohol. Zeolites No.s 1 (1% Cu/ZSM-5) , 2 (1.5% Cu/ZSM-5), 4 (1% Cu/NH4-ZSM-5), 7 (1% Fe/ZSM-5), 8 (1% Fe/MCM-41), 9 (1% Fe/SBA-15) gave no response under benzyl alcohol concentrations up to 200 µM. However, candidates No.s 5 (1% Cu/13X), 6 (1.5% Cu/Y), 10 (1% Mn/ZSM-5) also succeeded in giving a threshold shift in response to benzyl alcohol, similar as for zeolite No.3 (1% Cu/ZSM-5). All response characteristics ΔV_{th} *vs.* c for the benzyl alcohol- sensing zeolites are shown in Fig. 3:

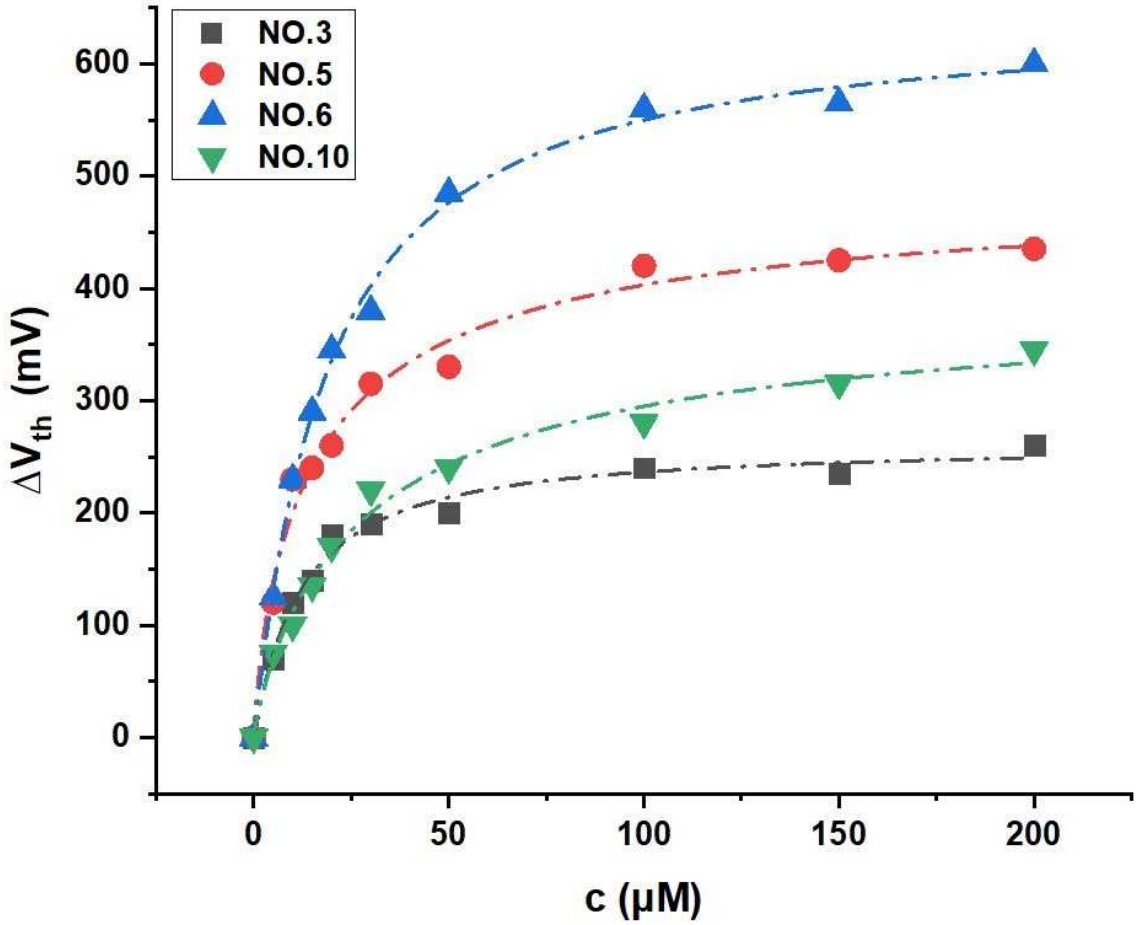

Fig. 3: Threshold shift ΔV_{th} *vs.* c in response to waterborne benzyl alcohol for WGTFTs sensitized with zeolites No.s 3, 5, 6, 10. The dashed lines are fits to eq. 1.

It is obvious that the characteristics in Fig.3 are not described by a Nikolsky Eisenman law (linear shift on log c scale for high c / flatlining for low c), as it is observed for ion selective WGTFTs using ion 'capturing' organic ionophores (Al Baroot and Grell 2019; Melzer et al. 2014; Schmoltner et al. 2013). Instead, the threshold shift increases steeply at low c but flatlines (saturates) at high c, as in (Alghamdi et al. 2019). Dashed lines are therefore fitted to a Langmuir- Freundlich (LF) adsorption isotherm, eq. 1, as described in section 2f, providing a good match to data. Resulting parameters and evaluated LoDs are listed in table 3:

Table 3: Characteristic parameters for fits of response characteristics, Fig. 3a, to LF model, eq. 1, for all zeolites that gave a threshold response to benzyl alcohol.

Zeolite No.	Substrate / Analyte	ΔV_{th}(sat) [mV]	K [10^4 L·mol^{-1}]	β	LoD [μM]
3	Benzyl alcohol	262 +/- 13	8.3 +/- 1.0	1.05 +/- 0.16	4.6
5	Benzyl alcohol	484 +/- 34	6.7 +/- 1.3	0.86 +/- 0.14	2.4
6	Benzyl alcohol	635 +/- 19	5.7 +/- 0.4	1.09 +/- 0.08	2.1
10	Benzyl alcohol	396 +/- 37	3.4 +/- 0.9	0.87 +/- 0.13	4.3

Here all K's are similar in the order a few 10^4 L·mol^{-1}, which is ~ 5 orders- of- magnitude smaller than K's for Cs^+ ion exchange with zeolite mordenite (Alghamdi et al. 2019). All four successful zeolites lead to benzyl alcohol- sensitive WGTFTs with LoDs of a few μM, 5 orders- of- magnitude lower than the concentration of a saturated benzyl alcohol solution in water (~ 370 mM at 25 °C (Lin et al. 2012)), and below the 'potability limit' (the concentration that should not be exceeded in water for human consumption) of 19 μM (Toxnet, BENZYL ALCOHOL). Saturated threshold shift is large, particularly for zeolite No. 6 - compare to 59 mV/decade for a Nernstian response law (Schmoltner et al. 2013), and the electrochemical window of water, 1230 mV. ΔV_{th}(sat) is similar or larger than for Cs^+ ion exchange with mordenite (Alghamdi et al. 2019). The threshold shift from surface adsorption of molecules carrying a dipole moment supports that the membrane potential developing in mordenite- sensitized membranes in response to Cs^+ also was due to interfacial dipoles. When comparing the surface areas of 'Zeolite Y', the support of catalyst No. 6, and 'ZSM-5', the support of catalysts No.s 3 and 5: Surface area of zeolite Y is given as 700 m^2 g^{-1} (Bortolatto et al. 2017), whereas for zeolite ZSM5 it is only 400

$m^2\ g^{-1}$ (Tortorelli et al 2014). The larger ΔV_{th}(sat) for catalyst No. 6 may therefore be due to larger surface area of Zeolite Y.

A clear correlation can be established between catalytic activity, as shown in table 1, and activity as benzyl alcohol sensitizer: Successful sensitizers 3, 5, 6 and 10 are also those with the highest catalytic conversion rates, above 0.15 $mM \cdot h^{-1}$. Zeolites with lower or no catalytic activity for benzyl alcohol also do not act as benzyl alcohol sensitizers. All protocols used to dope transition metal into the zeolite framework can lead to benzyl alcohol sensitivity - No. 3: DP; No.s 5, 10: WI; No. 6: IE all lead to benzyl alcohol sensitizers. Both Cu and Mn doped frameworks can lead to benzyl alcohol sensitizers. We found the strongest sensing response for zeolite No.6, which is also the only material that contains some Cu in oxidation state I (*cf.* supplementary section, S2b). Cu(I) is not essential though for catalytic activity nor sensor response, as successful catalysts / sensitizers No.s 3 (1% Cu/ZSM-5) and 5 (1% Cu/13X) contain Cu(II) only. The strong response for zeolite No. 6 may simply result from the larger surface area of 'parent' zeolite Y. However, there is no sensor response for Fe doped frameworks which also summarily failed as catalysts, *cf.* section 3a. Also, sensitizers are not limited to a specific Si : Al ratio, spanning 1.2 : 1 (No. 5) to 46 : 1 (No.s 3, 10). Frameworks MCM and SBA that lack Al altogether (No.s 8, 9) did not act as sensitizers, however this may be due to the doping with Fe only rather than a lack of Al.

c.) Attempted sensing of phenol and toluene

Following successful sensing of waterborne benzyl alcohol with WGTFTs, we have attempted to replicate a similar response for phenol. A number of catalysts were selected that are considered particularly promising: ZSM- 5 based zeolites show a high Si:Al ratio which is known to lead to a strong adsorption of phenols (Damjanović et al 2010 ; Khalid et al 2004), hence No.s 2,3,7 and 10 were tested. No. 2 is an active catalyst for phenol, No. 10 is almost inactive for phenol, *cf.* table 2. Further, No. 6 was tested for its good performance in benzyl alcohol sensors, albeit it shows low Si : Al ratio. However, while the catalytic activity for some of the zeolites selected here (*cf.* table 2) suggests good

adhesion of phenol very little or no threshold shift for WGTFTs sensitized was found for either of these catalysts. The most 'pronounced' response to phenol (Fig.4) was for No. 2, which is also among the most active catalysts for phenol degradation (table 2), but the threshold shift was still less than 80 mV even under 200 μM phenol. As phenol concentration in potable water should not exceed 35 μM (Babich et al. 1981 ; Summary of State and Federal Drinking Water Standards and Guidelines 1990), none of the zeolites studied here can lead to practical phenol sensors.

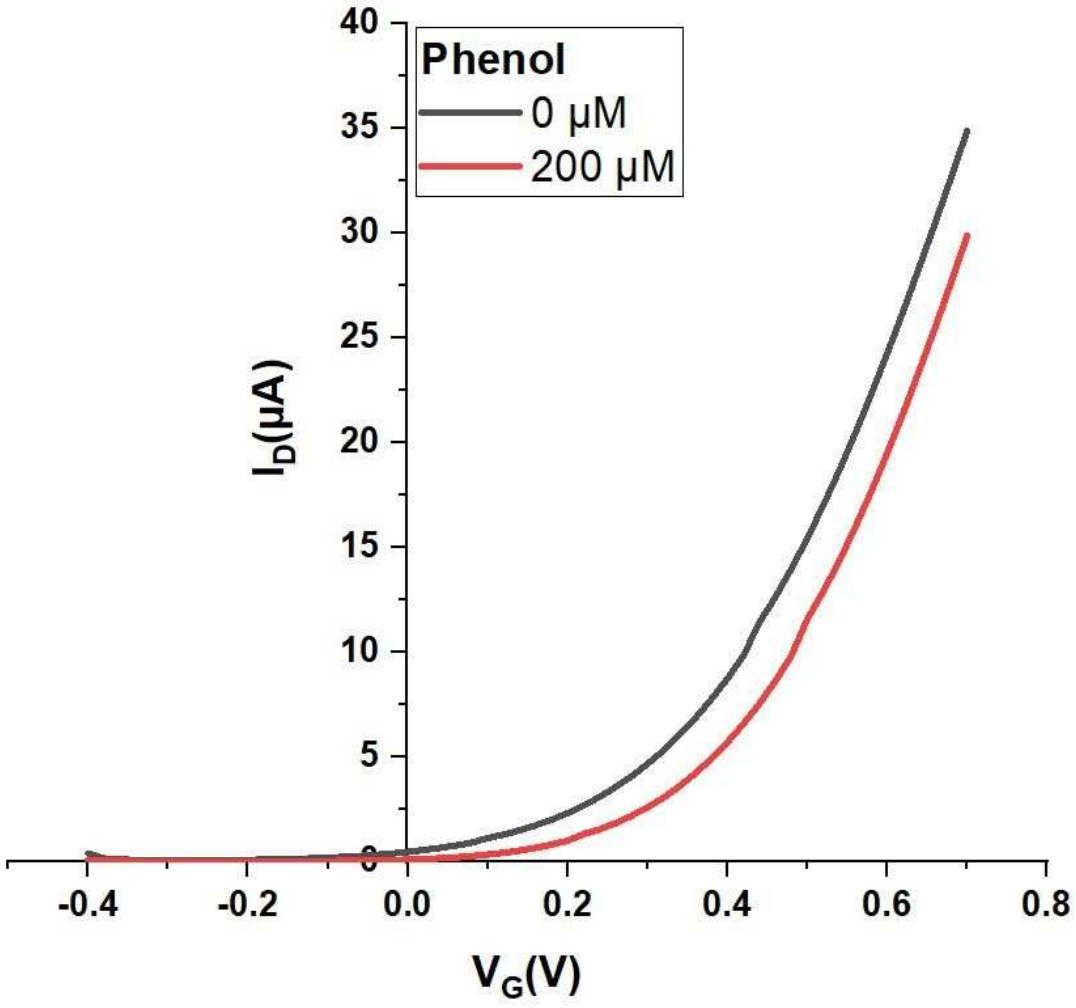

Fig. 4: Linear transfer characteristics for SnO_2 WGTFTs sensitized with zeolite No. 2 filled plasticized PVC membrane under pure water, and water with high concentration (200 μM) of phenol.

It is suggested that the lack of clear response to phenol comes from the different nature of its molecular dipole moment compared to benzyl alcohol: the dipole of phenol is locked in the plane of the aromatic ring as it is directly attached to it, while the dipole of benzyl alcohol is ‘free’, in the sense it is decoupled from the ring by a short saturated ‘spacer’ so it is not confined to the ring’s plane. Even if phenol can adsorb well onto catalyst, if adsorption is ‘face on’ onto catalyst surface, the dipole will be lateral (in the surface plane), and dipoles will cancel over an ensemble of many adsorbed phenols as they will be randomly orientated in the adsorption plane. WGTFT response to waterborne toluene on the example of catalysts No.s 5, 6, 10 has been also tested. These all showed a response to benzyl alcohol, and they represent different zeolite ‘families’: No. 5, based on zeolite type X, 6: Based on zeolite type Y, No. 10, based on ZSM5.

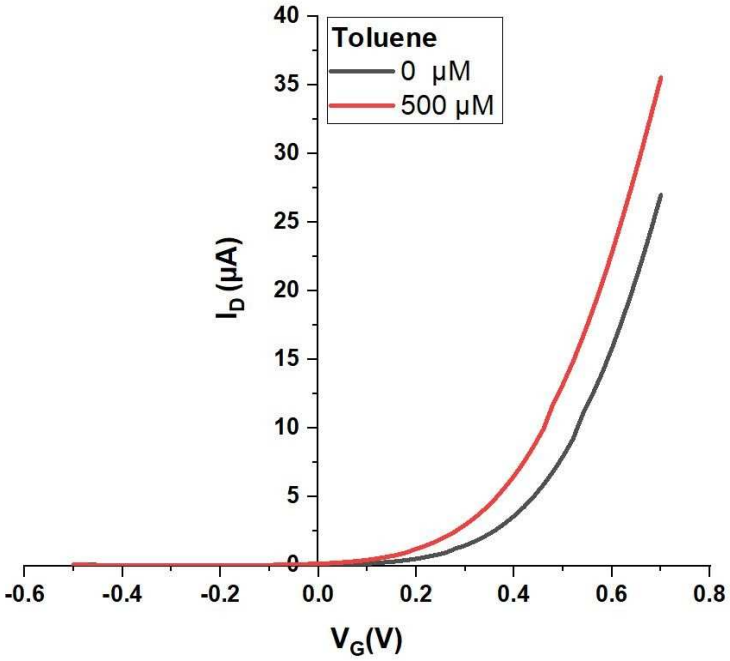
Toluene
0 μM
500 μM
I_D (μA)
V_G(V)
40
35
30
25
20
15
10
5
0
-0.6
-0.4
-0.2
0.0
0.2
0.4
0.6
0.8

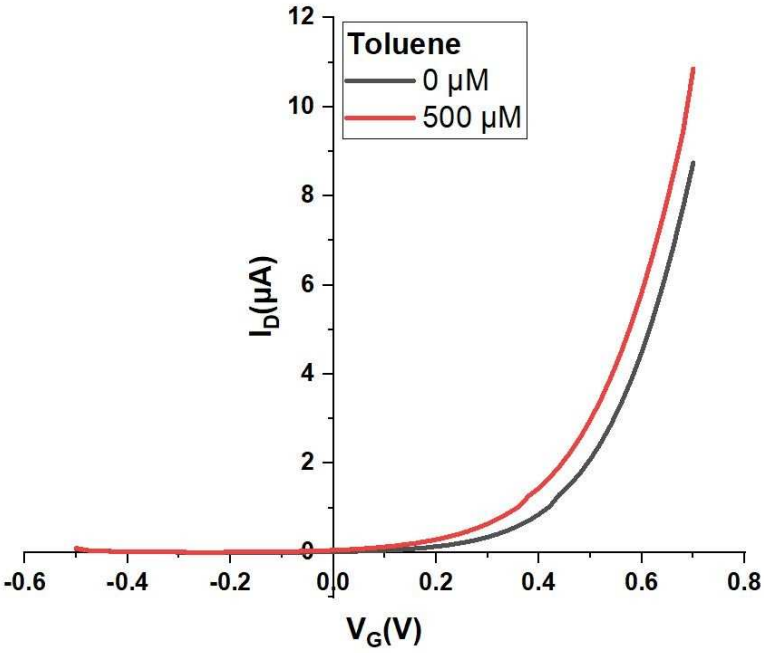
Toluene
0 μM
500 μM
I_D(μA)
V_G(V)
12
10
8
6
4
2
0
-0.6
-0.4
-0.2
0.0
0.2
0.4
0.6
0.8

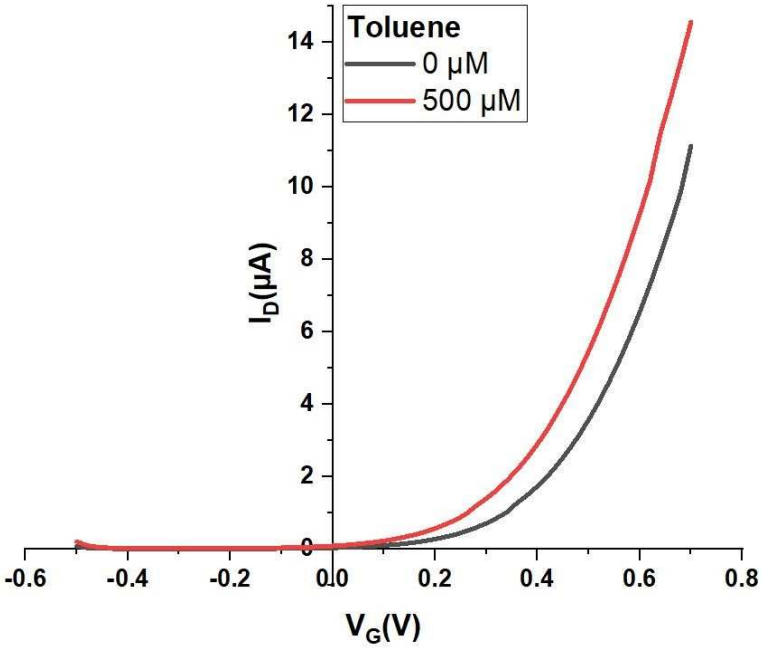

Fig. 5: Response of transfer characteristics of WGTFTs sensitized with zeolite 5 **(a)**, 6 **(b)**, and 10 **(c)**, to 500μM toluene.

However, even under 500 μM of toluene, which is far above the potability limit of 11 μM (Agency for Toxic Substances and Disease Registry 2017), the threshold shift does not exceed 70 mV, *cf.* Fig. 5. Toluene shows almost no molecular dipole, so even if it adsorbs well to catalyst surface, only little surface potential will develop. Also, the threshold shift is in the opposite direction than for benzyl alcohol, indicating reversed orientation of the (small) dipole moment or a screening effect of surface dipoles on the 'blank' zeolite sensitizer.

4. Conclusions

In conclusion, we demonstrated that when phase transfer membranes are appropriately sensitized, they can give a potentiometric response to relevant non-ionic aromatic solutes, that can be transduced with the WGTFT. This allows the sensing of aromatic water pollutant, benzyl alcohol, with a limit- of- detection (LoD) below its potability limit.

The observed potentiometric response is assigned to interfacial dipoles when an analyte with a ‘free’ molecular dipole (*i.e.* a dipole not locked in the molecular plain) adsorbs onto the surface of grains of powdered sensitizer. This is supported by the observed response characteristics that follow a Langmuir surface adsorption isotherm. The need for a ‘free’ molecular dipole makes our technique selective for potentiometric sensing for the application of non-symmetric or containing heteroatoms of aromatic pollutants in water, which although restricting its applicability, it nevertheless shows how sensing and catalytic activity can be bridged by the potentiometric sensor concept.

Identification of appropriate sensitizers for aromatic water pollutants was guided by a common prerequisite for both sensing, and heterogeneous catalysis: Both require adhesion of a ‘target’ pollutant molecule (*i.e.*, the analyte for sensing or the substrate for catalysis) on the surface of the sensitizer or catalyst. Therefore a number of transition metal doped zeolite- and related frameworks were tested as candidate sensitizers, because they are also considered as heterogeneous catalysts for the oxidation of the same pollutants. For benzyl alcohol, a clear correlation was established between ‘good’ catalysts (those with relatively high conversion rates) and successful sensitizers, namely the four candidates successful as sensitizers were those which displayed the highest catalytic activity. Attempted sensing of phenol was always unsuccessful though despite good catalytic activity for a number of zeolites studied here on phenol as substrate. It was these negative sensing results despite good catalytic activities that lead to the ‘free dipole’ criterion.

The present work provides a first example for the use of a catalyst as sensitizer in a phase transfer membrane for WGTFT potentiometric sensors. Hence, an application for catalysts was introduced that goes beyond catalysis, a concept that is recommended for more general consideration. The method established here can in principle also be used ‘in reverse’, namely to use potentiometry with the WGTFT to screen for promising candidate catalysts as a ‘shortcut’ from the labour-intensive procedure described in 2c. This will require detailed consideration of specific reactive pathways though, note *e.g.* the breakdown of phenol is by peroxide decomposition while oxidation of alcohols like benzyl

alcohol is via hydrogen abstraction (Weston et al. 2017). Potentiometric response signals surface adsorption only, without distinguishing later reactive pathways, and can only be applied for substrates with a 'free' dipole.

Acknowledgements

Nawal Alghamdi thanks the Cultural Attaché of Saudi Arabia to the UK and Tabuk University, Saudi Arabia, and Zahrah Alqahtani thanks the Cultural Attaché of Saudi Arabia to the UK and Taif University, Saudi Arabia, for providing them with fellowships for their Ph.D. studies. Changyan Zhou thanks the University of Sheffield and the Grantham Centre for Sustainable Futures for financial support.

Conflict of Interest: The authors declare that they have no conflict of interest

References:

Agency for Toxic Substances and Disease Registry, Toxicological Profile for Toluene, 4770 Buford Hwy NE, Atlanta, GA 30341 (2017). Available at: https://www.atsdr.cdc.gov/ToxProfiles/tp.asp?id=161&tid=29 (Accessed 8 Decemder 2019).

Al Baroot A.F, Grell M, (2019) Comparing electron-and hole transporting semiconductors in ion sensitive water-gated transistors. *Mater. Sci. Semicond. Process*. 89:216-222. https://doi.org/10.1016/j.mssp.2018.09.018

Alghamdi N, Alqahtani Z, Grell M, (2019) Sub-nanomolar detection of cesium with water-gated transistor. *J. Appl. Phys.,* 126(6): 064502. https://doi.org/10.1063/1.5108730

Alqahtani Z, Alghamdi N and M. Grell, (2020) Monitoring the lead- and- copper rule with a water- gated field effect transistor. *J. Water Health,*https://doi.org/10.2166/wh.2020.186

Arvand-Barmchi M, Mousavi M.F, Zanjanchi M.A, Shamsipur M, (2003) A PTEV-based zeolite membrane potentiometric sensor for cesium ion. *Sens. Actuators, B.,* 96(3): 560-564. https://doi.org/10.1016/S0925-4005(03)00639-7

Babich H, Davis D.L, (1981) Phenol: A review of environmental and health risks. *Regul. Toxicol. Pharmacol*. (1): 90-109. https://doi.org/10.1016/0273-2300(81)90071-4

Barrer R.M, Townsend R.P, Transition metal ion exchange in zeolites. Part 1. (1976) Thermodynamics of exchange of hydrated Mn^{2+}, Co^{2+}, Ni^{2+}, Cu^{2+} and Zn^{2+} ions in ammonium mordenite. *J. Chem. Soc., Faraday Trans,.1*: 72 661-673. DOI: 10.1039/F19767200661

Bortolatto L.B, Boca Santa R.A.A, Moreira J.C, Machado D.B, Martins M.A.P.M, Fiori M.A, Kuhnen N.C, Riella H.G, (2017) Synthesis and characterization of Y zeolites from alternative silicon and aluminium sources. *Micropor. Mesopor. Mater*. 248: 214-221. https://doi.org/10.1016/j.micromeso.2017.04.030

Brezinsky K, Litzinger T.A, Glassman I, (1984) The high temperature oxidation of the methyl side chain of toluene. *Int. J. Chem. Kin*. 16(9): 1053-1074. https://doi.org/10.1002/kin.550160902

Conte M, Lopez-Sanchez J.A, He Q, Morgan D.J, Ryabenkova Y, Bartley J.K, Carley A.F, Taylor S.H, Kiely C.J, Khalid K, Hutchings G.J, (2012) Modified zeolite ZSM-5 for the methanol to aromatics reaction. *Catal. Sci. Technol*., 2: 105-112. DOI: 10.1039/C1CY00299F

Damjanović L, Rakić V, Rac V, Stošić D, Auroux A, (2010) The investigation of phenol removal from aqueous solutions by zeolites as solid adsorbents. *J. Hazard. Mater.,* 184(1-3): 477-484. https://doi.org/10.1016/j.jhazmat.2010.08.059

Deroubaix G, Marcus P, (1992) X-ray photoelectron spectroscopy analysis of copper and zinc oxides and sulphides. *Surf. Interface Anal.*, 18:39. https://doi.org/10.1002/sia.740180107

Friend C.M, Xu B, (2017) Heterogeneous catalysis: a central science for a sustainable future. *Acc. Chem. Res.,* 50(3): 517-521. https://doi.org/10.1021/acs.accounts.6b00510

Gottlieb H.E, Kotlyar V, Nudelman A, (1997) NMR Chemical Shifts of Common Laboratory Solvents as Trace Impurities. *J. Org. Chem.,* 62:7512-7515. https://doi.org/10.1021/jo971176v

Gurbani A, Ayastuy J.L, González-Marcos M.P, Herrero J.E, Guil J.M, Gutiérrez-Ortiz M.A, (2009) Comparative study of $CuO–CeO_2$ catalysts prepared by wet impregnation and deposition–precipitation. *Int. J. Hydrog. Energy*, 34:547-553. https://doi.org/10.1016/j.ijhydene.2008.10.047

Inchaurrondo N.S, Massa P, Fenoglio R, Font J, Haure P. (2012) Efficient catalytic wet peroxide oxidation of phenol at moderate temperature using a high-load supported copper catalyst. *Chem. Eng. J*., 198-199: 426-434. https://doi.org/10.1016/j.cej.2012.05.103

Kergoat L, Herlogsson L, Braga D, Piro B, Pham M.C, Crispin X, Berggren M, Horowitz G. (2010) A water-gate organic field-effect transistor. *Adv. Mater*. 22(23):2565-2569.

https://doi.org/10.1002/adma.200904163

Khalid M, Joly G, Renaud A, Magnoux P, (2004) Removal of phenol from water by adsorption using zeolites. *Ind. Eng. Chem. Res.,* 43(17): 5275-5280.
https://doi.org/10.1021/ie0400447

Lin H.W, Yen C.H, Tan C.S, (2012) Aromatic hydrogenation of benzyl alcohol and its derivatives using compressed CO_2/water as the solvent. *Green Chem.,* 14(3): 682-687. DOI:10.1039/C2GC15999F

Lopez-Sanchez J. A, Conte M, Landon P, Zhou W, Bartley J. K, Taylor S. H, Carley A. F, Kiely J. C, Khalid K, Hutchings G. J (2012), Reactivity of Ga_2O_3 clusters on zeolite ZSM-5 for the conversion of methanol to aromatics, *Catal. Lett.*, 142 :1049-1056. DOI: 10.1007/s10562-012-0869-2

Ma S, Liu J, Li S, Chen B, Cheng J, Kuang J, Liu Y, Wan B, Wang Y, Ye J, Yu Q, Yuan W, Yu S, (2011) Development of a general and practical iron nitrate/TEMPO-catalyzed aerobic oxidation of alcohols to aldehydes/ketones: catalysis with table salt. *Adv. Synth. Catal*. 353: 1005-1017. https://doi.org/10.1002/adsc.201100033

Maduna Valkaj K, Katovic A, Zrnčević S, (2007) Investigation of the catalytic wet peroxide oxidation of phenol over different types of Cu/ZSM-5 catalyst. *J. Hazard. Mater.,* 144: 663-667. https://doi.org/10.1016/j.jhazmat.2007.01.099

Medford A.J, Vojvodic A, Hummelshøj J.S, Voss J, Abild-Pedersen F, Studt F, Bligaard T, Nilsson A, Nørskov J.K. (2015) From the Sabatier principle to a predictive theory of transition-metal heterogeneous catalysis. *J. Catal.,* 328: 36-42. https://doi.org/10.1016/j.jcat.2014.12.033

Melzer K, Münzer A.M, Jaworska E, Maksymiuk K, Michalska A, Scarpa G, (2014) Selective ion-sensing with membrane-functionalized electrolyte-gated carbon nanotube field-effect transistors. *Analyst,* 139(19): 4947-4954.DOI: 10.1039/C4AN00714J

Meng Y, Genuino H. C, Kuo C.-H, Huang H, Chen S.-Y, Zhang L, Rossi A, Suib S.L, (2013) One-Step hydrothermal synthesis of manganese-containing MFI-type zeolite, Mn-ZSM-5, characterization, and catalytic oxidation of hydrocarbons. *J. Am. Chem. Soc.,* 135(23): 8594-8605. https://doi.org/10.1021/ja4013936

Menon S.K, Modi N.R, Patel B, and Patel M.B, (2011) Azo calix [4] arene based neodymium (III)-selective PVC membrane sensor. *Talanta,* 83(5):1329-1334. https://doi.org/10.1016/j.talanta.2010.10.027

Nakamoto H, Takahashi H, (1981) Crystallization of Zeolite ZSM5 from single cation system, 10: 1739-1742. https://doi.org/10.1246/cl.1981.169

Polak J, and Lu B.C.Y. (1973) Mutual solubilities of hydrocarbons and water at 0 and 25 C. *Can. J. Chem.,* 51(24): 4018-4023. https://doi.org/10.1139/v73-599

Pople J.A, Gordon M, (1967) Molecular orbital theory of the electronic structure of organic compounds. I. Substituent effects and dipole moments, *J. Am. Chem. Soc,* 89(17): 4253-4261. https://doi.org/10.1021/ja00993a001

Rahman M.M, Abu-Zied B.M, Asiri A.M, (2018) Cu-loaded ZSM-5 zeolites: an ultra-sensitive phenolic sensor development for environmental safety. *J. Ind. Eng. Chem.,* 61: 304-313. https://doi.org/10.1016/j.jiec.2017.12.028

Rahman M.M, Abu-Zied B.M, Hasan M.M, Asiri A.M, and Hasnat M.A, (2016) Fabrication of a selective 4-amino phenol sensor based on H-ZSM-5 zeolites deposited silver electrodes. *RSC Adv.*, *6*(54): 48435-48444. https://doi.org/10.1039/C6RA04124H

Robert T, Offergeld G, (1972) Phys. Status Solidi A 14: 277-282.

Rostami S, Azizi S.N, Ghasemi S, (2017), Simultaneous electrochemical determination of hydrazine and hydroxylamine by CuO doped in ZSM-5 nanoparticles as a new amperometric sensor. *New J. Chem.*, *41*(22): 13712-13723. https://doi.org/10.1039/C7NJ02685D

Sahner K, Hagen G, Schönauer D., Reiß S, Moos R, (2008) Zeolites:Versatile materials for gas sensors. *Solid State Ionics*, *179*(40): 2416-2423. https://doi.org/10.1016/j.ssi.2008.08.012

Sankar C, Ponnuswamy V, Manickam M, Mariappan R, Suresh R, (2015) Structural, morphological, optical and gas sensing properties of pure and Ru doped SnO_2 thin films by nebulizer spray pyrolysis technique. *Appl. Surf. Sci.,* 349, 931-939. https://doi.org/10.1016/j.apsusc.2015.04.198

Schaefer T, Sebastian R, Peeling J, Penner G.H, Koh K, (1989) Conformational properties of benzyl alcohol in dilute solution. *Can. J. Chem*., 67(6): 1015-1021. https://doi.org/10.1139/v89-154

Schmoltner K, Kofler J, Klug A, List-Kratochvil E.J. (2013) Electrolyte-Gated Organic Field-Effect Transistor for Selective Reversible Ion Detection. *Adv. Mater.,* 25(47): 6895-6899.https://doi.org/10.1002/adma.201303281

Sigma-Aldrich,Silica,mesostructured MCM-41 type (hexagonal). [Online] Available at: https://www.sigmaaldrich.com/catalog/product/aldrich/643645?lang=en&region=GB (Accessed 19 September 2019).

Sigma-Aldrich,Silica,mesostructured SBA-15, 99% trace metals basis. [Online] Available at: https://www.sigmaaldrich.com/catalog/product/aldrich/777242?lang=en&region=GB (Accessed 19 September 2019).

Stinton G. W, Evans J. S. O, Parametric Rietveld refinement, J. Appl. Cryst., 40 (2007) 87-95. DOI: 10.1107/S0021889806043275

Summary of State and Federal Drinking Water Standards and Guidelines, United Sates Environmental Protection Agency, document EPA 570/R-90-019 (1990). Available at https://nepis.epa.gov/Exe/ZyNET.exe/10003I4B.TXT?ZyActionD=ZyDocument&Client=EPA&Index=1986+Thru+1990&Docs=&Query=&Time=&EndTime=&SearchMethod=1&TocRestrict=n&Toc=&TocEntry=&QField=&QFieldYear=&QFieldMonth=&QFieldDay=&IntQFieldOp=0&ExtQFieldOp=0&XmlQuery=&File=D%3A%5Czyfiles%5CIndex%20Data%5C86thru90%5CTxt%5C00000005%5C10003I4B.txt&User=ANONYMOUS&Password=anonymous&SortMethod=h%7C-&MaximumDocuments=1&FuzzyDegree=0&ImageQuality=r75g8/r75g8/x150y150g16/i425&Display=hpfr&DefSeekPage=x&SearchBack=ZyActionL&Back=ZyActionS&BackDesc=Results%20page&MaximumPages=1&ZyEntry=1&SeekPage=x&ZyPURL (Accessed 8 Decemder 2019).

ThermoFisher Scientific, 45866 Zeolite Y, hydrogen. [online] Available at:

https://www.alfa.com/en/catalog/045866/ (Accessed 20 August 2019).

ThermoFisher Scientific, 45879 zeolite ZSM-5 ammonuium. [online] Available at: https://www.alfa.com/en/catalog/045879/ . (Accessed 20 August 2019).

ThermoFisher Scientific, A10378 Molecular sieves, 13X, powder. [online] Available at: https://www.alfa.com/en/prodspec/A10378 (Accessed 20 August 2019)

Tortorelli, M, Landi G, Lisi L, Russo G, (2014) Adsorption and co-adsorption of NO and water on LaCu-ZSM5. *Micropor. Mesopor. Mater,* 200: 216-224. https://doi.org/10.1016/j.micromeso.2014.08.050

Toxnet.nlm.nih.gov. *BENZYL ALCOHOL - National Library of Medicine HSDB Database*, 2018 available at https://toxnet.nlm.nih.gov/cpdb/chempages/BENZYL%20ALCOHOL.html (Accessed 8 Decemder 2019).

Valkaj K.M, Katović A, Zrnčević S. (2011) Catalytic properties of Cu/13X zeolite based catalyst in catalytic wet peroxide oxidation of phenol. Ind. *Eng. Chem. Res,*. 50(8): 4390-4397. https://doi.org/10.1021/ie102223g

Weston J.O, Miyamura H, Yasukawa T, Sutarma D, Baker C.A, Singh P.K, Bravo-Sanchez M, Sano N, Cumpson P.J, Ryabenkova Y, Kobayashi S, Conte M, (2017) Water as a catalytic switch in the oxidation of aryl alcohols by polymer incarcerated rhodium nanoparticles *Catal. Sci. Technol*. 7: 3985-3998.DOI: 10.1039/C7CY01006K

Wilde C.A, Ryabenkova Y, Firth I.M, Pratt L, Railton J, Bravo-Sanchez M, Sano N, Cumpson P.J, Coates P.D, Liu X, Conte M, (2019). Novel rhodium on carbon catalysts for the oxidation of benzyl alcohol to benzaldehyde: A study of the modification of metal/support interactions by acid pre-treatments. *Appl. Catal. A: Gen,* 570: 271-282. https://doi.org/10.1016/j.apcata.2018.11.006

Xu B, Bordiga S, Prins R, van Bokhoven J.A, (2007) Effect of framework Si/Al ratio and extra-framework aluminum on the catalytic activity of Y zeolite. *Appl. Catal. A: Gen,*. 333: 245-253. https://doi.org/10.1016/j.apcata.2007.09.018

Zhao H, Neno T.M, Jennings G, Chupas P.J, Chapman K. W, (2011) Determining quantitative kinetics and the structural mechanism for particle growth in porous templates. *J. Phys. Chem. Lett,*. 2: 2742-2746. https://doi.org/10.1021/jz201260n

Čejka J, Morris R.E, Serrano D.P. (2016) Catalysis on zeolites, *Catal. Sci. Technol,*. 6: 2465-2466.DOI: 10.1039/C6CY90042A